Article

Discovery Medicine 2026; 38(212): 2990–3001
https://doi.org/10.24976/Discov.Med.202638212.230

SS-31 Attenuates Lipopolysaccharide-Induced Injury in HK-2 Renal Tubular Epithelial Cells via SIRT3-Mediated Regulation of Mitochondrial Metabolism

Xiangwei Wu[1], Menghan Shi[1], Min Sun[2], Zhiyong Xu[1], Hong Chen[1], Zhiqiang Hu[1], Jihui Ye[1,*]

[1]Department of Critical Care Medicine, The First Affiliated Hospital of Ningbo University, 315010 Ningbo, Zhejiang, China
[2]Central Laboratory, The First Affiliated Hospital of Ningbo University, 315010 Ningbo, Zhejiang, China
*Correspondence: yejihui78@163.com (Jihui Ye)
Submitted: 5 June 2026 Revised: 30 July 2026 Accepted: 10 August 2026 Published: 23 September 2026

Background: The mitochondrial-targeting peptide Elamipretide (SS-31) has shown protective effects against sepsis-associated acute kidney injury (S-AKI). Therefore, we investigated the mechanism underlying its effects on lipopolysaccharide (LPS)-induced injury in renal tubular epithelial cells, with a focus on mitochondrial lipid metabolism and the SIRT3-CPT2 signaling pathway.

Methods: Human renal proximal tubular epithelial (HK-2) cells were pretreated with different concentrations of SS-31, followed by exposure to LPS to establish an *in vitro* model of LPS-induced renal tubular injury. Cell viability and inflammatory cytokine levels were quantified by Cell Counting Kit-8 (CCK-8) and enzyme-linked immunosorbent assay (ELISA), respectively. Oxidative stress was determined through quantification of reactive oxygen species (ROS), malondialdehyde (MDA), and antioxidant enzyme activities. Mitochondrial membrane potential was detected using JC-1 staining, while intracellular lipid accumulation was assessed with BODIPY 493/503 staining. Fatty acid oxidation (FAO)-associated mitochondrial respiration was analyzed using a Seahorse XF Analyzer. Cell apoptosis was quantified by flow cytometry, and SIRT3 and CPT2 protein expressions were determined by Western blotting. Short hairpin RNA-mediated SIRT3 knockdown was performed to verify the mechanistic role of SIRT3.

Results: SS-31 increased LPS-treated HK-2 cell viability, and the effect was more significant at a concentration of 100 μM ($p < 0.01$). SS-31 intervention markedly downregulated inflammatory cytokines, ROS, and MDA while restoring antioxidant defenses ($p < 0.05$). In addition, SS-31 reduced intracellular lipid accumulation, altered mitochondrial oxygen consumption under FAO assay conditions, and decreased apoptosis ($p < 0.01$). Mechanistically, SS-31 markedly upregulated SIRT3 and CPT2 ($p < 0.05$). The knockdown of SIRT3 attenuated the protective effects of SS-31 and reduced the expression of CPT2 ($p < 0.05$), suggesting that the SIRT3-dependent regulation may be involved in the protective mechanism of SS-31.

Conclusion: SS-31 protects renal tubular epithelial cells against LPS-induced damage by modulating lipid metabolism and mitochondrial function through a SIRT3-dependent mechanism involving CPT2 regulation. These findings suggest its potential preventive utility and provide a mechanistic basis for further investigation in the context of S-AKI.

Keywords: SS-31; sepsis-induced acute kidney injury; sirtuin 3; lipid metabolism; mitochondrial function

Introduction

Sepsis, characterized by a maladjusted host response to infection that triggers systemic inflammatory response syndrome, represents a critical condition frequently leading to multiple organ dysfunction, septic shock, and elevated mortality rates [1]. In-hospital fatalities associated with this disorder range between 20% and 30% [2,3]. Among its severe complications, acute kidney injury (AKI) is highly prevalent, occurring in over 60% of septic patients and contributing significantly to their poor prognosis [4,5]. Clinically, AKI is identified by elevated serum creatinine concentrations and/or reduced urine output [6]. Although substantial research has been conducted to elucidate the pathogenesis of sepsis-induced AKI (S-AKI), its fundamental mechanisms are still not fully delineated. Microcirculatory impairment, inflammatory activation, and adaptive responses of renal tubular epithelial cells to injurious stimuli may play central roles [7,8]. Management currently emphasizes antibiotic therapy, infection source control, and supportive organ care [9]. Consequently, further investigation is warranted to develop novel therapeutic strategies and pharmacological interventions aimed at mitigating S-AKI.

Oxidative stress serves as a primary driver of AKI pathogenesis by inducing mitochondrial depolarization and impairing functional integrity [10,11,12]. Such dysfunction promotes inflammatory activation and facilitates the transition from AKI toward renal fibrosis [13,14]. Consequently, targeting mitochondrial impairment caused by oxidative stress represents a promising therapeutic strategy in sepsis-associated AKI [15]. Elamipretide (SS-31), a mitochondria-targeting tetrapeptide, can traverse cell membranes and selectively localize to the inner mitochondrial membrane, independently of the mitochondrial membrane potential (MMP) [16]. Its structure contains a dimethyltyrosine residue that confers antioxidant properties, enabling it to effectively scavenge reactive oxygen species (ROS) and suppress oxidation reactions [16,17]. By mitigating oxidative stress, this compound helps maintain mitochondrial bioenergetics, enhances ATP synthesis, and stabilizes MMP [17]. Although preclinical studies have demonstrated renoprotective effects of SS-31 in AKI models, its clinical efficacy in AKI remains to be established [18]. Moreover, the underlying antioxidant mechanisms through which it exerts protective effects in AKI remain to be fully elucidated.

S-AKI-associated genes were retrieved using GeneCards (https://www.genecards.org/) analysis. Mitochondria-related proteins were obtained from MitoCarta3.0 (https://www.broadinstitute.org/mitocarta/mitocarta30-inventory-mammalian-mitochondrial-proteins-and-pathways). The intersection between S-AKI-associated genes and mitochondrial protein datasets was performed using a Venn diagram analysis. The intersection of these datasets revealed carnitine palmitoyltransferase 2 (CPT2) as a candidate protein. CPT2 is involved in mitochondrial metabolism [19] and has been recognized as a protective factor in renal tubular inflammation [20]. Furthermore, CPT2 is regulated by sirtuin 3 (SIRT3), which enhances CPT2 enzymatic activity [21]. SIRT3 itself acts as a protective mediator in S-AKI [22]. Based on these findings, we hypothesize that SS-31 confers renal protection in S-AKI by modulating mitochondrial metabolism through a SIRT3-dependent mechanism involving CPT2 regulation.

Materials and Methods

Cell Culture and Transfection

HK-2 cells were purchased from AnWei-sci (AW-CH0140, Shanghai, China) and cultured in D-KSFM (AW-019, AnWei-sci) supplemented with 10% fetal bovine serum (FBS, AW-F0601, AnWei-sci) (37 °C, 5% CO_2). HK-2 cells were authenticated by short tandem repeat (STR) profiling and tested for mycoplasma contamination; all cells were confirmed to be mycoplasma-free.

The human SIRT3-targeting shRNA (shSIRT3, 5'-GCCCAACGTCACTCACTACTTT-3' (sense), 5'-AAAGTAGTGAGTGACGTTGGG-3' (antisense)) vector was constructed by RIBOBIO (ZT001, Guangzhou, China). Negative control shRNA (shNC, 5'-TTCTCCGAACGTGTCACGT-3' (sense), 5'-ACGTGACACGTTCGGAGAA-3' (antisense)) was also obtained from RIBOBIO. The vectors were transfected into HK-2 cells (1×10^4 cells per well) at 70–90% confluence using Lipofectamine 3000 (L3000150, Thermo Scientific, Waltham, MA, USA) and maintained for 48 h at 37 °C.

Quantitative Real-Time Polymerase Chain Reaction (qRT-PCR)

The knockdown efficiency of SIRT3 was verified by qRT-PCR. Following total RNA extraction from HK-2 cells (TRIzol reagent; 15596026, Thermo Scientific), reverse transcription was performed using a SuperScript™ VILO™ cDNA Synthesis Kit (11754250, Invitrogen, Carlsbad, CA, USA) following the instructions. Subsequently, qPCR was performed using a QuantStudio™ 7 Pro system with SYBR Green-based master mix (4385612, Thermo Scientific) and SIRT3 primer (sense: 5'-ATTCCAGACTTCAGATCG-3'; antisense: 5'-GAAAGTAGTGAGTGACGTTG-3') or β-actin primer (sense: 5'-CAAATGCTTCTAGGCGGACTATG-3'; antisense: 5'-TGCGCAAGTTAGGTTTTGTCA-3'). Amplification conditions were as follows: 95 °C (20 s); 95 °C (3 s); and 60 °C (30 s) for 40 cycles. Relative mRNA expression level was analyzed via the $2^{-\Delta\Delta CT}$ method, with β-actin as the reference gene.

Cell Treatment

Untransfected or transfected HK-2 cells were pretreated with 50 or 100 μM SS-31 for 2 h [23], followed by treatment with 1 μg/mL lipopolysaccharide (LPS; L8880, Solarbio, Beijing, China) [24] for 24 h. Cells were then collected for subsequent assays.

Cell Counting Kit-8 (CCK-8) Assay

After HK-2 cells (5×10^3 cells per well) were treated with LPS or/and SS-31, 10 μL/well of WST-8 reagent (ab228554, Abcam, Cambridge, UK) was added, and the mixture incubated for 4 h under light-protected conditions. The absorbance (460 nm) was subsequently examined with a CytoSMART Omni multimode microplate reader (Axion BioSystems, Shanghai, China).

Enzyme-Linked Immunosorbent Assay (ELISA)

Interleukin 1β (IL-1β, ab214025), IL-6 (ab178013), tumor necrosis factor-α (TNF-α, ab181421), and monocyte chemoattractant protein-1 (MCP-1, ab179886) levels in cell culture supernatants were quantified using ELISA kits (Abcam). Briefly, 50 μL of samples or standards were added to 96-well plates and incubated with 50 μL of the corresponding antibodies for 1 h. After washing, 100 μL of tetramethylbenzidine (TMB) substrate was added for 10 min for color development. The reaction was stopped with Stop Solution, and absorbance was measured at 450 nm.

Oxidative Stress Determination

Intracellular ROS levels were assessed via DCFH-DA fluorescence (D6883, Sigma-Aldrich, St. Louis, MO, USA). Briefly, cells were loaded with 10 μM DCFH-DA (37 °C, 30 min). Fluorescence was recorded on a microplate reader (excitation/emission = 504/529 nm) and expressed as relative fluorescence units (RFU).

Malondialdehyde (MDA) content, reflecting lipid peroxidation, was assessed using an MDA assay kit (MAK085, Sigma-Aldrich). Absorbance (532 nm) was measured and normalized to total protein concentration. Results are presented as nmol per mg protein.

Superoxide dismutase (SOD) activity was determined with a WST-8-based SOD assay kit (19160, Sigma-Aldrich). The reduction rate of WST-8 was monitored at 450 nm. SOD activity was calculated and expressed as units per mg protein.

Glutathione peroxidase (GSH-Px) activity was evaluated using a coupled enzymatic reaction assay kit (CGP1, lot number: 0000397879, Sigma-Aldrich). The absorbance decrease at 340 nm was recorded, and activity was normalized to protein content. Results are given in units per mg protein.

Mitochondrial Membrane Potential (MMP)

The JC-1 Assay Kit (C2003S, Beyotime, Shanghai, China) was used to evaluate MMP. HK-2 cells (2×10^6 cells/mL) were seeded and allowed to adhere. Following incubation, cells were stained with JC-1 working solution (20 min, 37 °C). After staining, the cells were washed twice and resuspended in cold assay buffer. The MMP of the cells was detected using flow cytometry. The gating strategy was as follows: cells were first gated on the FSC-A vs. SSC-A plot to exclude debris and select the main cell population. Doublets were then excluded by FSC-A vs. FSC-H gating to analyze single cells. JC-1 fluorescence was detected in the FL-1 channel (green, JC-1 monomers) and FL-2 channel (red, JC-1 aggregates). The percentage of cells with mitochondrial depolarization (green, JC-1 monomers) was quantified.

BODIPY 493/503 Staining

HK-2 cells grown on glass coverslips underwent fixation and culture with 2 μM BODIPY-493/503 staining solution (V42795, InvivoChem, Guangzhou, China) (15 min, 37 °C, darkness). After washing, the cells were stained with DAPI. Coverslips were then mounted, and fluorescence images were captured using an inverted fluorescence microscope at 200× magnification. The BODIPY positive area was quantified using ImageJ software (1.52a; National Institutes of Health, Bethesda, MD, USA).

Seahorse Assay

XF96 Analyzer (Agilent, Santa Clara, CA, USA) was used to measure cellular oxygen consumption rate (OCR). For mitochondrial stress tests, OCR was assessed after sequential injection of oligomycin (1.5 μM, HY-N6782, MedChemExpress, Princeton, NJ, USA), FCCP (1 μM, HY-100410, MedChemExpress), and rotenone/antimycin A (0.5 μM, HY-107406, MedChemExpress). For fatty acid oxidation (FAO) assays, cells were preconditioned in Seahorse substrate-limited medium overnight, then treated with etomoxir (40 μM), palmitate-BSA (200 μM) or BSA (200 μM) before OCR measurement under the same inhibitor regimen. FAO-associated OCR was calculated as the difference in OCR between palmitate-BSA-treated wells and etomoxir-treated wells. Following Seahorse analysis, the assay medium was removed, and cells were washed twice with phosphate-buffered saline (PBS, P1003, Solarbio, Beijing, China) prior to lysis. Total protein content was measured using a BCA quantification kit (PC0020, Solarbio, Beijing, China). All OCR values were normalized to total protein.

Cell Apoptosis Assay

Following treatment, both floating and adherent cells were collected. Adherent cells were gently detached using 0.25% trypsin (without EDTA, 40124ES60, Yeasen, Shanghai, China) and combined with the floating cells to avoid loss of apoptotic cells. After centrifugation and washing with cold PBS, cells (1×10^5 cells per tube) were mixed with Annexin V-FITC and PI staining solution (5 μL each) in an apoptosis detection kit (MA0220, Meilunbio, Dalian, China), followed by incubation (15 min, room temperature, darkness). Analysis was carried out within 1 h on a flow cytometer (CytoFLEX, Beckman Coulter, Brea, CA, USA). Quantification of apoptotic populations was performed using CytExpert software (version 2.2; Beckman Coulter, Brea, CA, USA). The gating strategy was as follows: cells were first gated on the FSC-A vs. SSC-A plot to exclude debris and select the main cell population. Doublets were then excluded by FSC-A vs. FSC-H gating. Annexin V-FITC fluorescence was detected in the FL-1 channel and PI fluorescence in the FL-2 channel. Based on Annexin V and PI staining patterns, four populations were distinguished: viable cells (Annexin V^-/PI^-), early apoptotic cells (Annexin V^+/PI^-), late apoptotic cells (Annexin V^+/PI^+), and necrotic cells (Annexin V^-/PI^+). The percentage of apoptotic cells was calculated as the sum of early and late apoptotic populations.

Western Blotting

Total cellular proteins were extracted with radioimmunoprecipitation assay (RIPA, PC101, Epizyme, Shanghai, China) buffer supplemented with a protease inhibitor (B14001, Selleck, Shanghai, China) and quantified by a BCA kit. Following heating at 95 °C for 5 min in load-

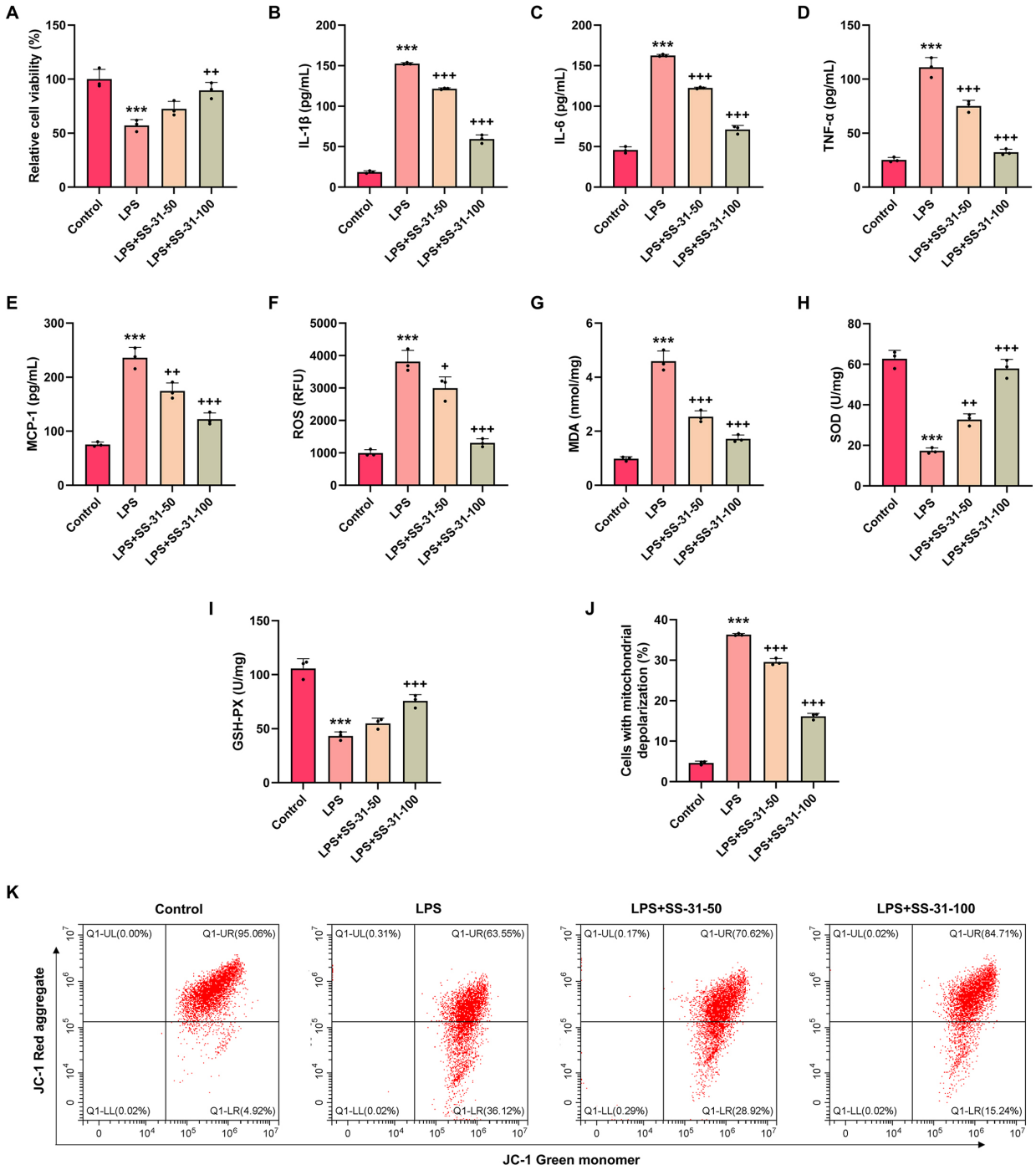

Fig. 1. SS-31 ameliorates LPS-induced injury in renal tubular epithelial cells. HK-2 cells were pretreated with 50 μM or 100 μM SS-31 and then stimulated with LPS to establish injury models. (A) Cell viability (CCK-8 assay). (B–E) Inflammatory cytokine levels of IL-1β, IL-6, TNF-α, and MCP-1 (ELISA). (F–I) Oxidative stress parameters ROS, MDA, SOD, and GSH-Px (assay kits). (J,K) MMP (flow cytometry with JC-1 staining). n = 3. $^{***}p < 0.001$ vs. Control; $^{+}p < 0.05$, $^{++}p < 0.01$, $^{+++}p < 0.001$ vs. LPS. SS-31, Elamipretide; LPS, lipopolysaccharide; IL-1β, Interleukin 1β; CCK-8, Cell Counting Kit-8; TNF-α, tumor necrosis factor-α; MCP-1, monocyte chemoattractant protein-1; ROS, reactive oxygen species; MDA, malondialdehyde; SOD, superoxide dismutase; GSH-Px, glutathione peroxidase.

ing buffer, proteins were electrophoresed on NuPAGE™ 4–12% Bis-Tris precast gels (NP0321BOX, Thermo Fisher Scientific) and subsequently transferred onto polyvinylidene difluoride (PVDF) membranes (YA1701, Solarbio). The membranes were blocked with 5% non-fat milk and probed with primary antibodies (Abcam) (4 °C, overnight):

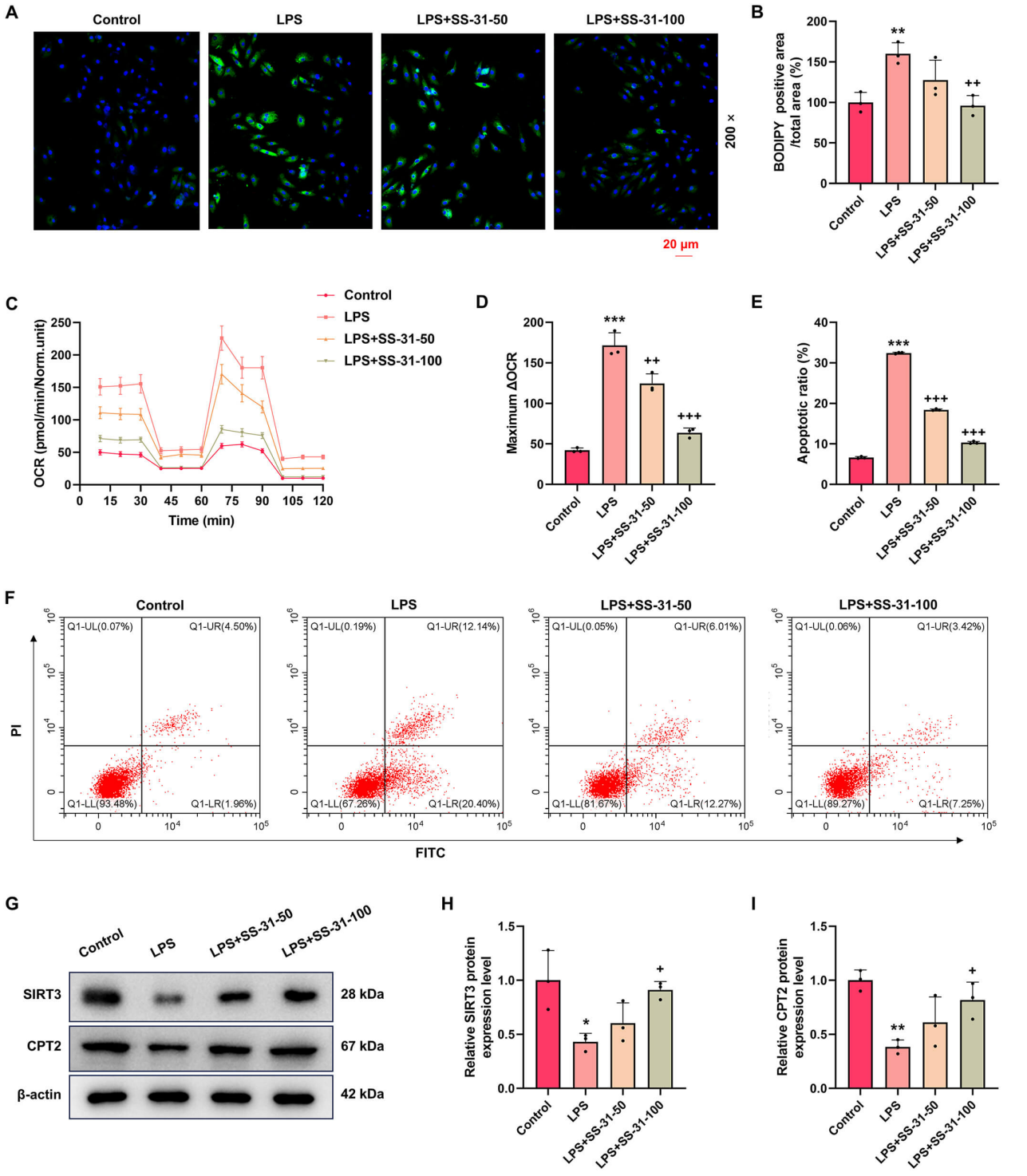

Fig. 2. SS-31 attenuates lipid accumulation and apoptosis, alters FAO-associated OCR, and upregulates SIRT3 and CPT2 expression. HK-2 cells were pretreated with 50 μM or 100 μM SS-31 and then stimulated with LPS to establish injury models. (A,B) Lipid droplet accumulation (BODIPY 493/503 staining). (C,D) OCR under FAO assay conditions (Seahorse XF Analyzer). (E,F) Apoptosis (flow cytometry with Annexin V/PI staining). (G–I) SIRT3 and CPT2 protein levels (Western blotting). n = 3. $^{*}p < 0.05$, $^{**}p < 0.01$, $^{***}p < 0.001$ vs. Control; $^{+}p < 0.05$, $^{++}p < 0.01$, $^{+++}p < 0.001$ vs. LPS. OCR, oxygen consumption rate; FAO, fatty acid oxidation.

SIRT3 (ab217319, 1:1000), CPT2 (ab181114, 1:1000), and β-actin (ab8226, 1:10,000). The membranes were then washed with TBST and incubated for 1 h with secondary antibodies, either anti-rabbit (ab175781, Abcam; 1:10,000) or anti-mouse (ab205719, Abcam; 1:10,000). Blots were visualized with BeyoECL Plus chemilumines-

cent substrate (P0018S, Beyotime) and captured using an iBright CL750 imaging system (A44116, Thermo Fisher Scientific, Waltham, MA, USA). Protein expressions were normalized to β-actin.

Statistical Analyses

Quantitative data are expressed as means ± SD from three biologically independent replicates. The Shapiro-Wilk normality test was used to test normality. One-way analysis of variance (ANOVA) was used for intergroup comparisons, followed by Tukey's Honest Significant Difference. A p-value < 0.05 was defined as statistically significant. Image processing and quantitative analyses were carried out using ImageJ software.

Results

SS-31 Ameliorates LPS-Induced Injury in Renal Tubular Epithelial Cells

To dissect how SS-31 influences LPS-triggered cell damage, we first assessed cell viability by CCK-8 assay. As exhibited in Fig. 1A, LPS significantly reduced HK-2 cell viability ($p < 0.001$), while 100 μM SS-31 intervention restored cell viability ($p < 0.01$). We next quantified key inflammatory cytokines using ELISA. Compared with only the LPS treatment group, SS-31 markedly reduced the secretion of IL-1β, IL-6, TNF-α, and MCP-1 (Fig. 1B–E; $p < 0.01$). Furthermore, oxidative stress parameters were evaluated. SS-31 treatment attenuated ROS/MDA production while upregulating SOD and GSH-Px (antioxidant enzymes) activities in LPS-induced cells (Fig. 1F–I; $p < 0.05$). MMP determination indicated that SS-31 effectively attenuated LPS-induced mitochondrial depolarization (Fig. 1J,K; $p < 0.001$).

SS-31 Reduces Lipid Accumulation and FAO-Associated Mitochondrial Respiration While Suppressing Apoptosis

Given the critical roles of lipotoxicity and mitochondrial dysfunction in S-AKI, we further assessed lipid accumulation using BODIPY 493/503 staining. SS-31 reduced lipid droplet accumulation (green) in LPS-stimulated HK-2 cells, as evidenced by the decreased BODIPY-positive area following SS-31 treatment (Fig. 2A,B; $p < 0.01$). Using the Seahorse XF Analyzer, we found that SS-31 decreased the basal and maximal OCR under FAO assay conditions in LPS-induced cells (Fig. 2C,D; $p < 0.01$). Additionally, flow cytometric analysis revealed that SS-31 markedly suppressed LPS-induced apoptosis (Fig. 2E,F; $p < 0.001$). Western blot analysis further demonstrated that SIRT3 and CPT2 were inhibited by LPS treatment (Fig. 2G–I; $p < 0.05$), while SS-31 upregulated their protein expression (Fig. 2G–I; $p < 0.05$), suggesting a potential mechanism involving the SIRT3-CPT2 pathway.

Knockdown of SIRT3 Reverses the Protective Effects of SS-31

To clarify the role of SIRT3 in the protective effects of SS-31, we established a SIRT3-knockdown HK-2 cell model using shRNA transfection. Knockdown efficiency was confirmed by qRT-PCR (Fig. 3A, $p < 0.001$) and Western blotting (Fig. 3B,C, $p < 0.001$). In SIRT3-deficient cells, the promotive effect of SS-31 on cell viability was abolished (Fig. 3D; $p < 0.01$). Moreover, the anti-inflammatory effects of SS-31 were reversed, as indicated by upregulated IL-1β, IL-6, TNF-α, and MCP-1 (Fig. 3E–H; $p < 0.001$). Similarly, the antioxidant effects of SS-31 were compromised in SIRT3-knockdown cells (Fig. 4A–D; $p < 0.01$). The mitochondrial protective effect of SS-31 was also attenuated by SIRT3 knockdown, as evidenced by increased mitochondrial depolarization and decreased MMP (Fig. 4E,F; $p < 0.001$).

SIRT3 Knockdown Attenuates the Effects of SS-31 on Lipid Metabolism, FAO-Associated Mitochondrial Respiration, and Apoptosis

We further explored the role of SIRT3 in SS-31-mediated regulation of lipid metabolism. As illustrated in Fig. 4G,H, SIRT3 knockdown abolished the reduction in lipid droplets (green) induced by SS-31, as evidenced by the increased BODIPY-positive area ($p < 0.05$). Consistent with this, the inhibitory effect of SS-31 on OCR under FAO assay conditions was significantly attenuated in SIRT3-knockdown cells (Fig. 5A,B; $p < 0.001$). Flow cytometric analysis also showed that SIRT3 knockdown restored the apoptotic rate that was reduced by SS-31 (Fig. 5C,D; $p < 0.001$). According to Western blotting, CPT2 expression, upregulated by SS-31, was decreased in SIRT3-knockdown cells (Fig. 5E,F; $p < 0.05$).

Discussion

Herein, we establish that SS-31, a mitochondrial-targeting peptide, effectively protected renal tubular epithelial cells against LPS-induced injury by modulating lipid metabolism and mitochondrial function, which is a SIRT3-dependent mechanism involving CPT2. Our findings reveal a previously unrecognized mechanism by which SS-31 ameliorates LPS-induced renal tubular damage, highlighting its potential therapeutic utility, particularly in a prophylactic context, for sepsis-associated renal damage.

As reviewed by Zhu et al. [18], SS-31 exerts renoprotective effects by preserving mitochondrial function, reducing oxidative stress, and maintaining mitochondrial homeostasis. However, the involvement of mitochondrial lipid metabolism in SS-31-mediated renal protection has yet to be pinpointed. Here, we further demonstrated that SS-31 regulates lipid metabolism through a SIRT3-dependent mechanism involving CPT2 in LPS-injured renal tubular epithelial cells, broadening the current understanding of its

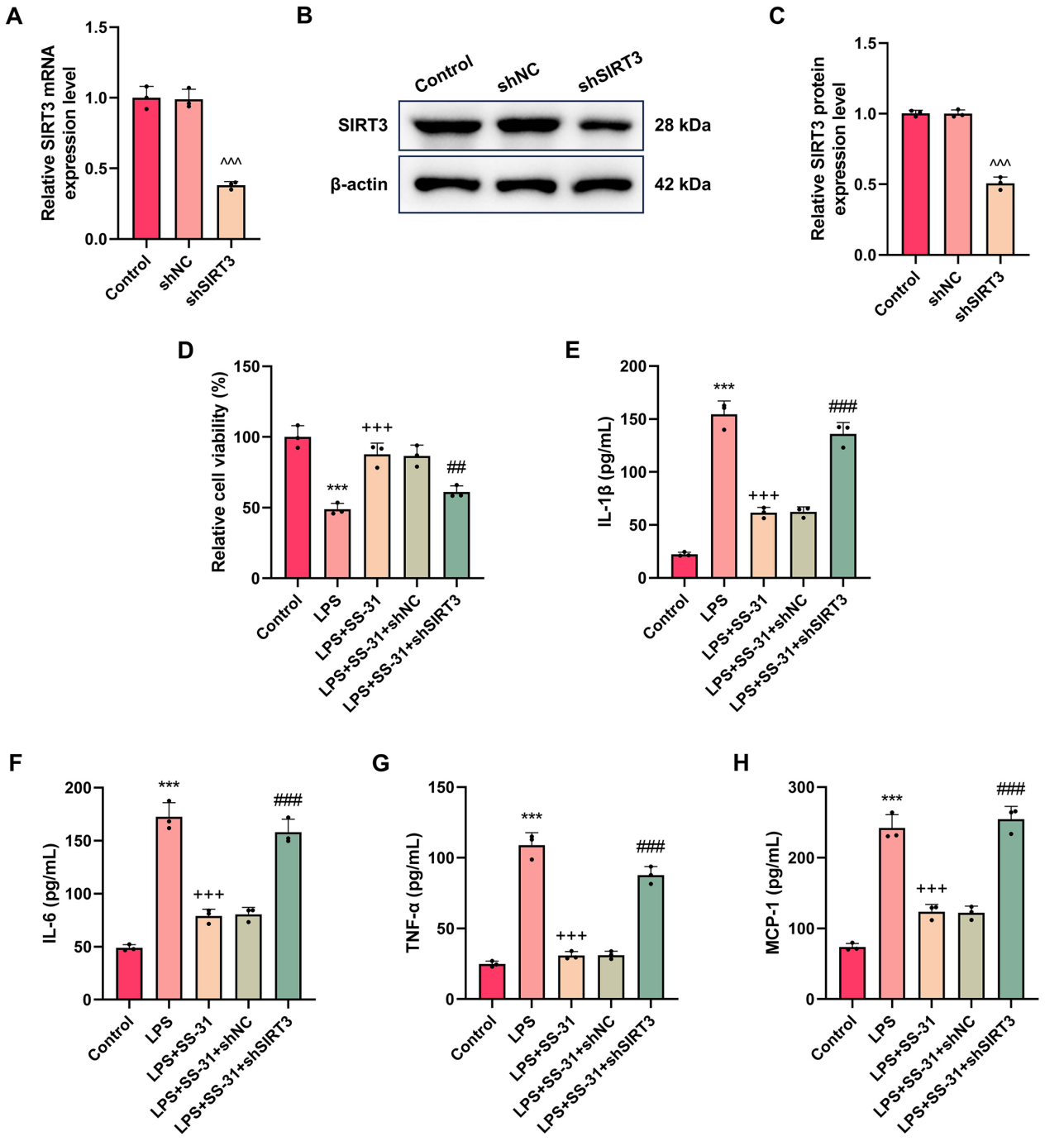

Fig. 3. SIRT3 knockdown reverses the protective effects of SS-31 on LPS-induced inflammation. HK-2 cells were transfected with shSIRT3 to knock down SIRT3 expression, pretreated with SS-31 and subsequently exposed to LPS. (A–C) Efficient SIRT3 knockdown in HK-2 cells (qRT-PCR and Western blot analysis). (D) Cell viability (CCK-8 assay). (E–H) Inflammatory cytokines (ELISA). n = 3. $^{\wedge\wedge\wedge}p < 0.001$ vs. shNC; $^{***}p < 0.001$ vs. Control; $^{+++}p < 0.001$ vs. LPS. $^{\#\#}p < 0.01$, $^{\#\#\#}p < 0.001$ vs. LPS + SS-31 + shNC.

mechanism. The antioxidant function of SS-31 benefits from its localization within the mitochondrial inner membrane and its potent ROS scavenging capacity, which underlies its strong therapeutic efficacy in AKI. In a rat model of renal ischemic injury, Szeto et al. [25] demonstrated that SS-31 significantly improved renal function and ameliorated tubular damage following renal ischemia-reperfusion. A further mechanistic study revealed that this protection is closely associated with the preservation of mitochondrial structure and function, thereby alleviating oxidative stress and inflammatory responses in renal tubular epithelial cells [25]. Consistent with these findings, our study in an *in vitro*

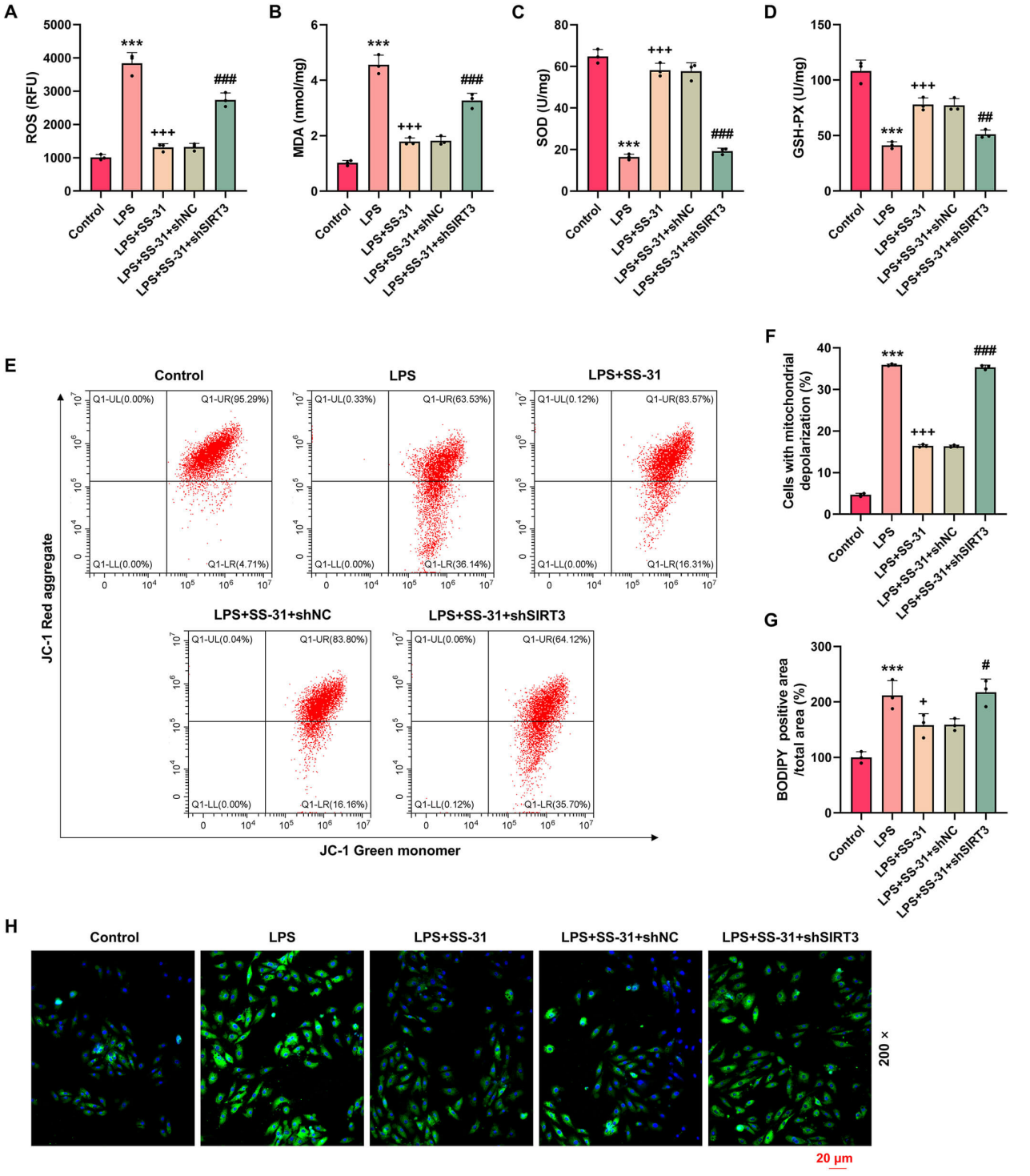

Fig. 4. SIRT3 knockdown reverses the protective effects of SS-31 on LPS-induced oxidative stress, mitochondrial dysfunction, and lipid metabolism. HK-2 cells were transfected with shSIRT3 to knock down SIRT3 expression, pretreated with SS-31 and subsequently exposed to LPS. (A–D) Oxidative stress markers. (E,F) MMP (JC-1 staining). (G,H) Lipid droplet accumulation (BODIPY 493/503 staining). n = 3. $^{***}p < 0.001$ vs. Control; $^{+}p < 0.05$, $^{+++}p < 0.001$ vs. LPS. $^{\#}p < 0.05$, $^{\#\#}p < 0.01$, $^{\#\#\#}p < 0.001$ vs. LPS + SS-31 + shNC.

model of LPS-induced injury also showed that SS-31 reduces levels of ROS, MDA, and inflammatory cytokines, while increasing antioxidant enzyme activity. Particularly noteworthy is its promotive effect on MMP, suggesting that SS-31 mitigates LPS-induced oxidative stress and inflammatory injury in renal tubular epithelial cells by restoring mitochondrial structure and function.

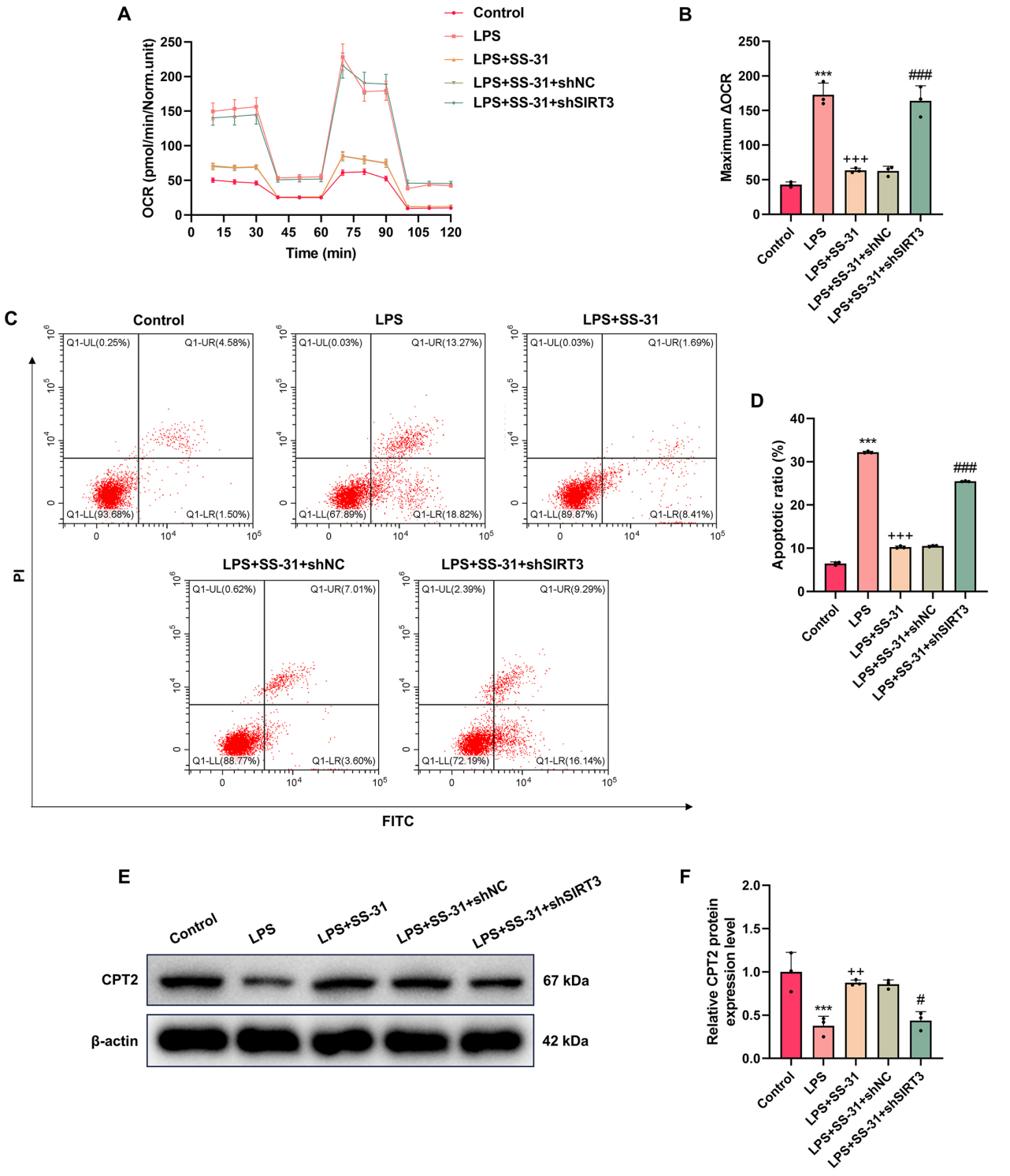

Fig. 5. SIRT3 knockdown attenuates the effects of SS-31 on FAO-associated OCR, apoptosis, and CPT2 expression. HK-2 cells were transfected with shSIRT3 to knock down SIRT3 expression, pretreated with SS-31 and subsequently exposed to LPS. (A,B) OCR under FAO assay conditions (Seahorse XF Analyzer). (C,D) Apoptosis (flow cytometry). (E,F) CPT2 protein expression (Western blotting). n = 3. $^{***}p < 0.001$ vs. Control; $^{++}p < 0.01$, $^{+++}p < 0.001$ vs. LPS. $^{\#}p < 0.05$, $^{\#\#\#}p < 0.001$ vs. LPS + SS-31 + shNC.

Interestingly, our findings showed that SS-31 reduced lipid accumulation and altered mitochondrial oxygen consumption under FAO assay conditions in LPS-stimulated renal tubular cells. This observation contradicts the conventional understanding that impaired FAO is a key pathological feature of S-AKI, given that FAO serves as a critical

energy source for renal tissues and is compromised during sepsis due to hypoxia [26]. On the other hand, excessive ROS production has been shown to enhance mitochondrial FAO, which in turn increases renal vascular permeability and compromises barrier function [27]. This conclusion is further supported by findings in diabetic models, where accelerated cardiac FAO renders the heart more susceptible to ischemic injury [28]. Importantly, although CPT2 expression was increased in SS-31-treated cells, this does not necessarily indicate enhanced FAO flux, as FAO is regulated at multiple levels including substrate availability, mitochondrial redox status, and enzymatic coupling efficiency, rather than CPT2 expression alone. Moreover, Seahorse OCR-based measurements reflect FAO-associated oxygen consumption indirectly and cannot fully represent true FAO flux. Therefore, changes in OCR should be interpreted as functional readouts of mitochondrial respiration rather than direct evidence of FAO rate. Direct FAO flux assays were not performed in the present study, which limits definitive conclusions regarding FAO activity. Therefore, the reduced OCR observed under FAO assay conditions in SS-31-treated cells might represent an adaptive mechanism that limits excessive ROS generation and prevents mitochondrial membrane depolarization. Our data suggest that SS-31 exerts its protective effects through strategic metabolic reprogramming rather than a generalized enhancement of mitochondrial function.

Our study further identified SIRT3 as a key mediator of SS-31. SIRT3, a major mitochondrial NAD+-dependent deacetylase, governs energy metabolism and antioxidant defense [29]. We found that SS-31 significantly upregulated SIRT3 expression and that SIRT3 knockdown attenuated the beneficial effects of SS-31 on cell viability, inflammation, oxidative stress, and lipid metabolism, highlighting the importance of SIRT3 activation in SS-31-mediated protection. Previous studies have shown that SIRT3 deficiency exacerbates organ injury in various disease models, especially in AKI [30,31,32], while SIRT3 activation protects against mitochondrial dysfunction [33]. Our study extends these findings by demonstrating that SS-31 exerts its effects in a manner that is at least partially dependent on SIRT3 activation, providing a specific molecular target for future therapeutic interventions.

Notably, we discovered that SS-31 increased CPT2 expression in a SIRT3-dependent manner. CPT2 is a critical enzyme in mitochondrial FAO that facilitates the transport of long-chain fatty acids into the mitochondrial matrix [34]. The positive regulatory role of SIRT3 on CPT2 has been extensively documented in numerous studies. For instance, the SIRT3-CPT2 axis modulates lipid metabolism in bovine hepatocytes, preventing triglyceride accumulation [35]. SIRT3 maintains mitochondrial homeostasis and functionality by stabilizing CPT2, thereby promoting cell proliferation [36,37]. While SS-31 reduced overall OCR under FAO assay conditions, it simultaneously upregulated CPT2 expression, suggesting a complex regulatory mechanism that may involve compartmentalization of lipid metabolism or feedback regulation.

Several limitations warrant consideration. First, our data were derived solely from *in vitro* cell line experiments, which makes it difficult to reflect the complexity of S-AKI *in vivo*. Future studies using animal models of sepsis will be necessary to validate these findings. Second, the precise mechanism by which SS-31 upregulates SIRT3 expression remains unclear and warrants further investigation. Third, the experimental grouping for mechanistic validation was limited. We did not include key control groups such as LPS+shSIRT3 (without SS-31), SS-31+shSIRT3 (without LPS), or shSIRT3 alone. Consequently, our data demonstrate that SIRT3 knockdown attenuates the observed effects of SS-31, but are insufficient to conclusively prove that the effects of SS-31 are entirely dependent on SIRT3. Fourth, while we focused on CPT2 as a downstream effector, other SIRT3 targets may also contribute to the observed effects.

Despite these limitations, our study provides compelling evidence that SS-31 protects renal tubular epithelial cells against LPS-induced damage by SIRT3-mediated regulation of lipid metabolism and mitochondrial function. Given the limited treatment options currently available for S-AKI, these findings support SS-31 as a promising candidate for further preclinical investigation, particularly in exploring its prophylactic potential and therapeutic efficacy in more complex *in vivo* models. Future studies should explore its effects in animal models of sepsis and further elucidate the role of mitochondrial lipid metabolism in mediating its protective effects.

Conclusion

In summary, we demonstrate that SS-31 attenuates LPS-induced injury in renal tubular epithelial cells by modulating lipid metabolism and mitochondrial function through a SIRT3-dependent mechanism involving CPT2 regulation. These findings suggest its potential preventive utility, and not only deepen our understanding of S-AKI pathogenesis but also identify potential molecular targets for further investigation in the context of sepsis-associated acute kidney injury.

Availability of Data and Materials

The datasets used or analyzed during the current study are available from the corresponding author upon reasonable request.

Author Contributions

XWW, MHS and JHY designed the research study; XWW, MS, ZYX and HC performed the research; ZYX, MS, HC and ZQH collected and analyzed the data. XWW,

MHS, ZQH and JHY have been involved in drafting the manuscript and all authors have been involved in revising it critically for important intellectual content. All authors gave final approval of the version to be published. All authors have participated sufficiently in the work to take public responsibility for appropriate portions of the content and agreed to be accountable for all aspects of the work in ensuring that questions related to its accuracy or integrity.

Ethics Approval and Consent to Participate

Not applicable.

Acknowledgment

Not applicable.

Funding

This work was supported by the Medical and Health Science and Technology Program of Zhejiang Province [grant number: 2024KY330] and the Traditional Chinese Medicine Science and Technology Program of Zhejiang Province [grant number: 2024ZL915].

Conflict of Interest

The authors declare no conflict of interest.

References

[1] Singer M, Deutschman CS, Seymour CW, Shankar-Hari M, Annane D, Bauer M, et al. The Third International Consensus Definitions for Sepsis and Septic Shock (Sepsis-3). JAMA. 2016; 315: 801–810. https://doi.org/10.1001/jama.2016.0287

[2] Angus DC, van der Poll T. Severe sepsis and septic shock. The New England Journal of Medicine. 2013; 369: 840–851. https://doi.org/10.1056/NEJMra1208623

[3] Cecconi M, Evans L, Levy M, Rhodes A. Sepsis and septic shock. Lancet (London, England). 2018; 392: 75–87. https://doi.org/10.1016/S0140-6736(18)30696-2

[4] Poston JT, Koyner JL. Sepsis associated acute kidney injury. BMJ (Clinical Research Ed.). 2019; 364: k4891. https://doi.org/10.1136/bmj.k4891

[5] Russell JA, Singer J, Bernard GR, Wheeler A, Fulkerson W, Hudson L, et al. Changing pattern of organ dysfunction in early human sepsis is related to mortality. Critical Care Medicine. 2000; 28: 3405–3411. https://doi.org/10.1097/00003246-200010000-00005

[6] Koeze J, Keus F, Dieperink W, van der Horst ICC, Zijlstra JG, van Meurs M. Incidence, timing and outcome of AKI in critically ill patients varies with the definition used and the addition of urine output criteria. BMC Nephrology. 2017; 18: 70. https://doi.org/10.1186/s12882-017-0487-8

[7] Peerapornratana S, Manrique-Caballero CL, Gómez H, Kellum JA. Acute kidney injury from sepsis: current concepts, epidemiology, pathophysiology, prevention and treatment. Kidney International. 2019; 96: 1083–1099. https://doi.org/10.1016/j.kint.2019.05.026

[8] Tang L, Zhou F, Wang Y, Jiao Y. The E3 Ubiquitin Ligase MIB2 Exacerbates Sepsis-Associated Acute Kidney Injury by Promoting GPX4 Degradation-Mediated Ferroptosis and Mitochondrial Dysfunction. Discovery Medicine. 2025; 37: 2041–2054. https://doi.org/10.24976/Discov.Med.202537200.175

[9] Gotts JE, Matthay MA. Sepsis: pathophysiology and clinical management. BMJ (Clinical Research Ed.). 2016; 353: i1585. https://doi.org/10.1136/bmj.i1585

[10] van der Slikke EC, Star BS, van Meurs M, Henning RH, Moser J, Bouma HR. Sepsis is associated with mitochondrial DNA damage and a reduced mitochondrial mass in the kidney of patients with sepsis-AKI. Critical Care (London, England). 2021; 25: 36. https://doi.org/10.1186/s13054-020-03424-1

[11] Ommati MM, Farshad O, Azarpira N, Shafaghat M, Niknahad H, Heidari R. Betaine alleviates cholestasis-associated renal injury by mitigating oxidative stress and enhancing mitochondrial function. Biologia. 2020; 76: 351–365. https://doi.org/10.2478/s11756-020-00576-x

[12] Li J, Zhang H. Protective Effects of Propofol on Acute Kidney Injury Through Suppressing Ferroptosis and Inflammatory Responses in Renal Tubular Epithelial Cells. Discovery Medicine. 2025; 37: 3095–3106. https://doi.org/10.24976/Discov.Med.202537203.259

[13] Son SS, Jeong HS, Lee SW, Lee ES, Lee JG, Lee JH, et al. EPRS1-mediated fibroblast activation and mitochondrial dysfunction promote kidney fibrosis. Experimental & Molecular Medicine. 2024; 56: 2673–2689. https://doi.org/10.1038/s12276-024-01360-6

[14] Wu YJ, Yang YR, Yan YL, Yang HY, Du JR. Targeting mitochondrial dysfunction: an innovative strategy for treating renal fibrosis. Molecular and Cellular Biochemistry. 2025; 480: 4889–4906. https://doi.org/10.1007/s11010-025-05297-w

[15] Tang L, Zhang J, Han J, Zhang D, Zhang H, Liu J, et al. Molecular mechanism of circHIPK3 in mitochondrial function in septic acute kidney injury. Environmental Toxicology. 2024; 39: 2596–2609. https://doi.org/10.1002/tox.24127

[16] Tung C, Varzideh F, Farroni E, Mone P, Kansakar U, Jankauskas SS, et al. Elamipretide: A Review of Its Structure, Mechanism of Action, and Therapeutic Potential. International Journal of Molecular Sciences. 2025; 26: 944. https://doi.org/10.3390/ijms26030944

[17] Du X, Zeng Q, Luo Y, He L, Zhao Y, Li N, et al. Application research of novel peptide mitochondrial-targeted antioxidant SS-31 in mitigating mitochondrial dysfunction. Mitochondrion. 2024; 75: 101846. https://doi.org/10.1016/j.mito.2024.101846

[18] Zhu Y, Luo M, Bai X, Li J, Nie P, Li B, et al. SS-31, a Mitochondria-Targeting Peptide, Ameliorates Kidney Disease. Oxidative Medicine and Cellular Longevity. 2022; 2022: 1295509. https://doi.org/10.1155/2022/1295509

[19] Liu L, Xie B, Fan M, Candas-Green D, Jiang JX, Wei R, et al. Low-Level Saturated Fatty Acid Palmitate Benefits Liver Cells by Boosting Mitochondrial Metabolism via CDK1-SIRT3-CPT2 Cascade. Developmental Cell. 2020; 52: 196–209.e9. https://doi.org/10.1016/j.devcel.2019.11.012

[20] Wang M, Wang L, Zhou L, Xu Y, Wang C. Shen-Shuai-II-Recipe inhibits tubular inflammation by PPARα-mediated fatty acid oxidation to attenuate fibroblast activation in fibrotic kidneys. Phytomedicine : International Journal of Phytotherapy and Phytopharmacology. 2024; 126: 155450. https://doi.org/10.1016/j.phymed.2024.155450

[21] Li M, Li D, Wang HY, Zhang W, Zhuo Z, Guo H, et al. Leptin decreases Th17/Treg ratio to facilitate neuroblastoma via inhibiting long-chain fatty acid catabolism in tumor cells. Oncoimmunology. 2025; 14: 2460281. https://doi.org/10.1080/2162402X.2025.2460281

[22] Fan H, Le JW, Sun M, Zhu JH. Sirtuin 3 deficiency promotes acute kidney injury induced by sepsis *via* mitochondrial dysfunction and apoptosis. Iranian Journal of Basic Medical Sci-

ences. 2021; 24: 675–681. https://doi.org/10.22038/ijbms.2021.54905.12312

[23] Yang SK, Han YC, He JR, Yang M, Zhang W, Zhan M, et al. Mitochondria targeted peptide SS-31 prevent on cisplatin-induced acute kidney injury via regulating mitochondrial ROS-NLRP3 pathway. Biomedicine & Pharmacotherapy = Biomedecine & Pharmacotherapie. 2020; 130: 110521. https://doi.org/10.1016/j.biopha.2020.110521

[24] Li XJ, Liu T, Wang Y. Allicin ameliorates sepsis-induced acute kidney injury through Nrf2/HO-1 signaling pathway. Journal of Natural Medicines. 2024; 78: 53–67. https://doi.org/10.1007/s11418-023-01745-3

[25] Szeto HH, Liu S, Soong Y, Wu D, Darrah SF, Cheng FY, et al. Mitochondria-targeted peptide accelerates ATP recovery and reduces ischemic kidney injury. Journal of the American Society of Nephrology : JASN. 2011; 22: 1041–1052. https://doi.org/10.1681/ASN.2010080808

[26] Gómez H. Reprogramming Metabolism to Enhance Kidney Tolerance during Sepsis: The Role of Fatty Acid Oxidation, Aerobic Glycolysis, and Epithelial De-Differentiation. Nephron. 2023; 147: 31–34. https://doi.org/10.1159/000527392

[27] Shu Z, Chen S, Xiang H, Wu R, Wang X, Ouyang J, et al. AKT/PACS2 Participates in Renal Vascular Hyperpermeability by Regulating Endothelial Fatty Acid Oxidation in Diabetic Mice. Frontiers in Pharmacology. 2022; 13: 876937. https://doi.org/10.3389/fphar.2022.876937

[28] Karwi QG, Sun Q, Lopaschuk GD. The Contribution of Cardiac Fatty Acid Oxidation to Diabetic Cardiomyopathy Severity. Cells. 2021; 10: 3259. https://doi.org/10.3390/cells10113259

[29] Feng J, Feng L, Yan Y, Ye H, Tang K, Guo X, et al. SIRT3 deficiency aggravates mitochondrial metabolic disorder and podocyte injury in DKD via MPC2 acetylation. Cellular Signalling. 2025; 135: 112029. https://doi.org/10.1016/j.cellsig.2025.112029

[30] Cheng L, Yang X, Jian Y, Liu J, Ke X, Chen S, et al. SIRT3 deficiency exacerbates early-stage fibrosis after ischaemia-reperfusion-induced AKI. Cellular Signalling. 2022; 93: 110284. https://doi.org/10.1016/j.cellsig.2022.110284

[31] Locatelli M, Macconi D, Corna D, Cerullo D, Rottoli D, Remuzzi G, et al. Sirtuin 3 Deficiency Aggravates Kidney Disease in Response to High-Fat Diet through Lipotoxicity-Induced Mitochondrial Damage. International Journal of Molecular Sciences. 2022; 23: 8345. https://doi.org/10.3390/ijms23158345

[32] Song S, Ding Y, Dai GL, Zhang Y, Xu MT, Shen JR, et al. Sirtuin 3 deficiency exacerbates diabetic cardiomyopathy via necroptosis enhancement and NLRP3 activation. Acta Pharmacologica Sinica. 2021; 42: 230–241. https://doi.org/10.1038/s41401-020-0490-7

[33] Kim JE, Jo MJ, Bae SY, Ahn SY, Ko GJ, Kwon YJ. Mitochondrial SIRT3 as a protective factor against cyclosporine A-induced nephrotoxicity. Scientific Reports. 2024; 14: 10143. https://doi.org/10.1038/s41598-024-60453-4

[34] Pereyra AS, Rajan A, Ferreira CR, Ellis JM. Loss of Muscle Carnitine Palmitoyltransferase 2 Prevents Diet-Induced Obesity and Insulin Resistance despite Long-Chain Acylcarnitine Accumulation. Cell Reports. 2020; 33: 108374. https://doi.org/10.1016/j.celrep.2020.108374

[35] Liu L, Xing D, Du X, Peng T, McFadden JW, Wen L, et al. Sirtuin 3 improves fatty acid metabolism in response to high nonesterified fatty acids in calf hepatocytes by modulating gene expression. Journal of Dairy Science. 2020; 103: 6557–6568. https://doi.org/10.3168/jds.2019-17670

[36] Song S, Yang M, Li J, Li Y, Wang L, Yao S, et al. SIRT3 mediates CPT2 delactylation to enhance mitochondrial function and proliferation in goat granulosa cells. Journal of Animal Science and Biotechnology. 2025; 16: 101. https://doi.org/10.1186/s40104-025-01231-8

[37] Xie B, Liu L, Candas-Green D, Fan M, Jiang J, Wei R, et al. Low level saturated fatty acid palmitate benefits liver cells by boosting mitochondrial homeostasis via CDK1-SIRT3-CPT2 cascade. Free Radical Biology and Medicine. 2018; 128: S96. https://doi.org/10.1016/j.freeradbiomed.2018.10.227